Technology
Collaboration
Programme
by iea

IEA EOR TCP

// STAVANGER 2022

ANNUAL EVENT

21 – 24 Nov

eor

Enhanced Oil Recovery

New Development in Modelling of Viscous Fingering

Arne Skauge, Ken Sorbie, Alan Beteta, Tormod Skauge, Eric Mackay

Energy Research Norway and Heriot-Watt University, UK

Dynamic reservoir characterization

STAVANGER 2022
ANNUAL EVENT
21 – 24 Nov

IEA EOR TCP

eor
Enhanced Oil Recovery

The Mobility Equations

Phase Mobilities

$$\lambda_o = \left(k_{ro} / \mu_o \right)$$

$$\lambda_w = \left(k_{rw} / \mu_w \right)$$

$$\lambda_T = \lambda_w + \lambda_o$$

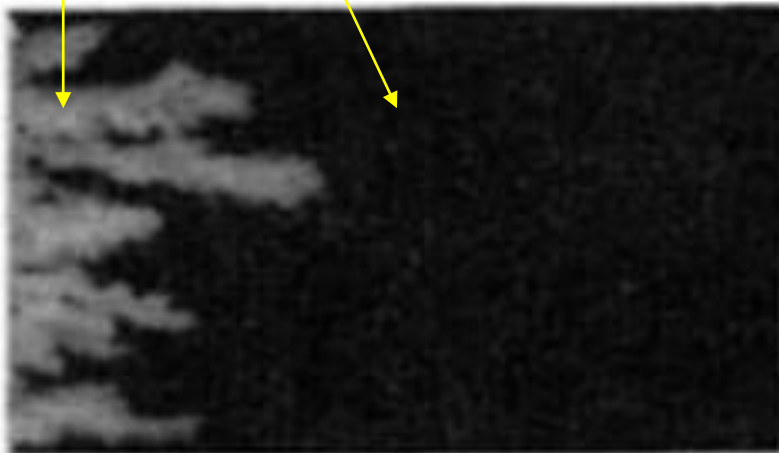Mobility Ratio

$$M\left(S_w \right) = \left(\lambda_w / \lambda_o \right)$$

One of the Earliest Published Examples of Immiscible Viscous Fingering van Meurs and van der Poel (1958)

"Viscous fingering" = Engleberts and Klinkenberg (1951)

$$(\mu_o / \mu_w) = 80$$
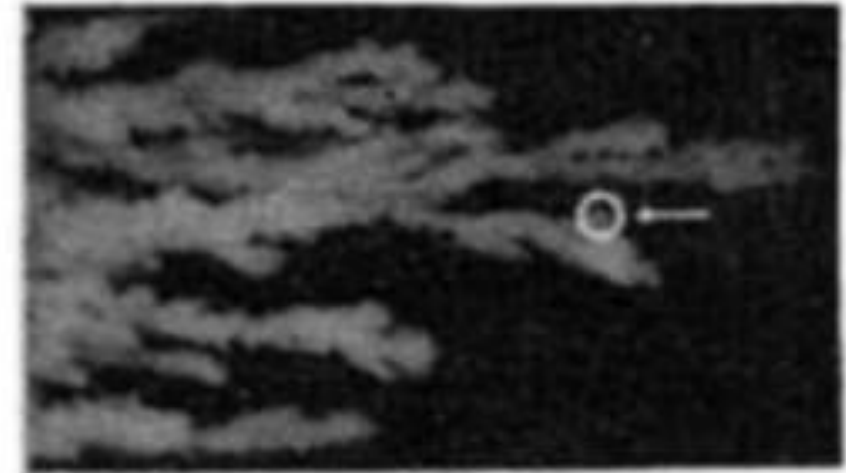
Water → Oil

(a) N_p = 0.06   (b) N_p = 0.095   (c) N_p = 0.12

Figure 1: Immiscible viscous fingering of water (white fluid) displacing oil (dark fluid) in a high permeability 2D pack with ; from van Meurs and van der Poel (1958). N_p is the number of PV injection of the water phase.

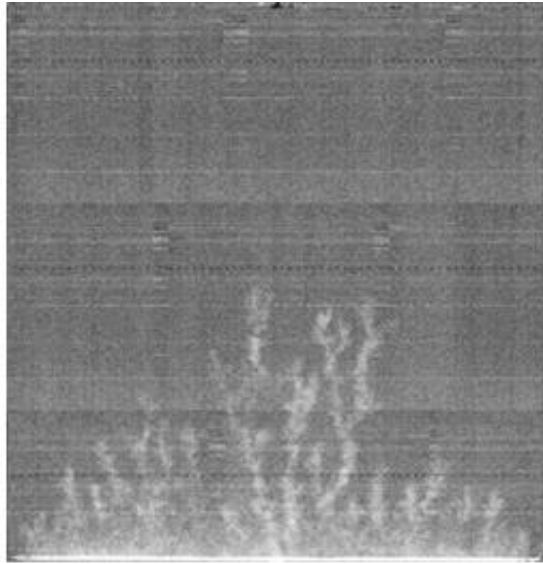# Recent Work by Skauge and Coworkers ~2010 –
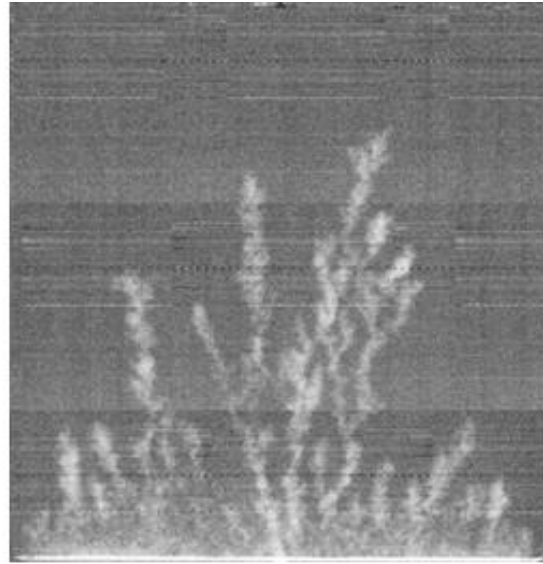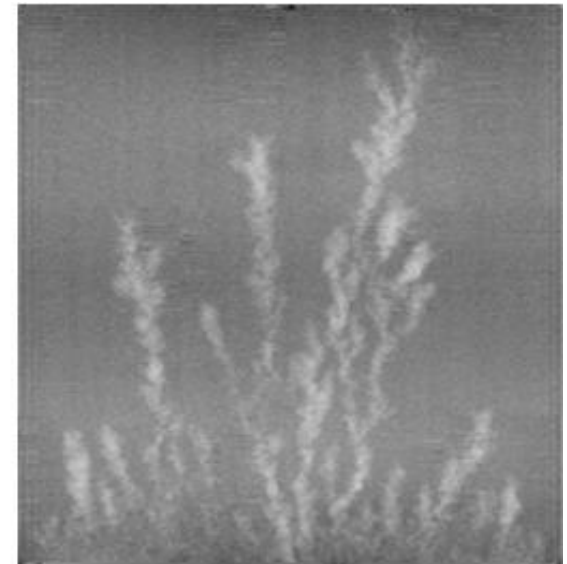
Experimental – 2D X-Ray scanner

N
Slab (1) Statoil
2

Top View

Detector/camera

Sample

X-ray

Window

Doors
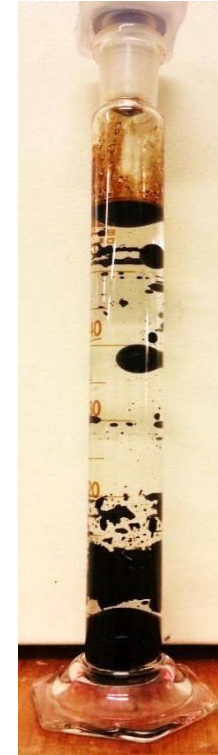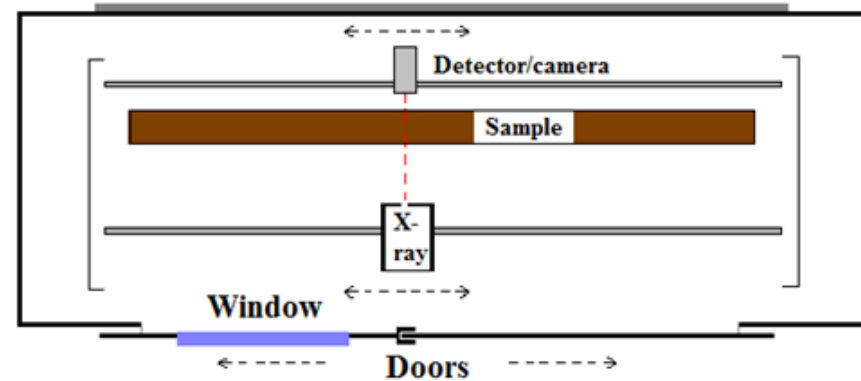
Waterflood E2000

0.01 PV   0.02 PV   0.04 PV
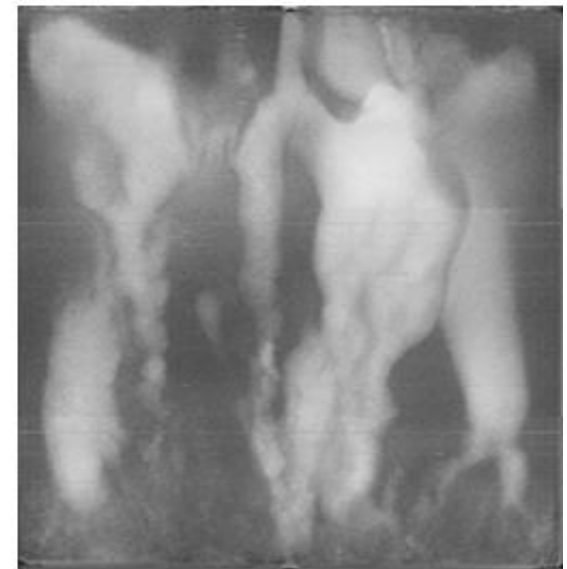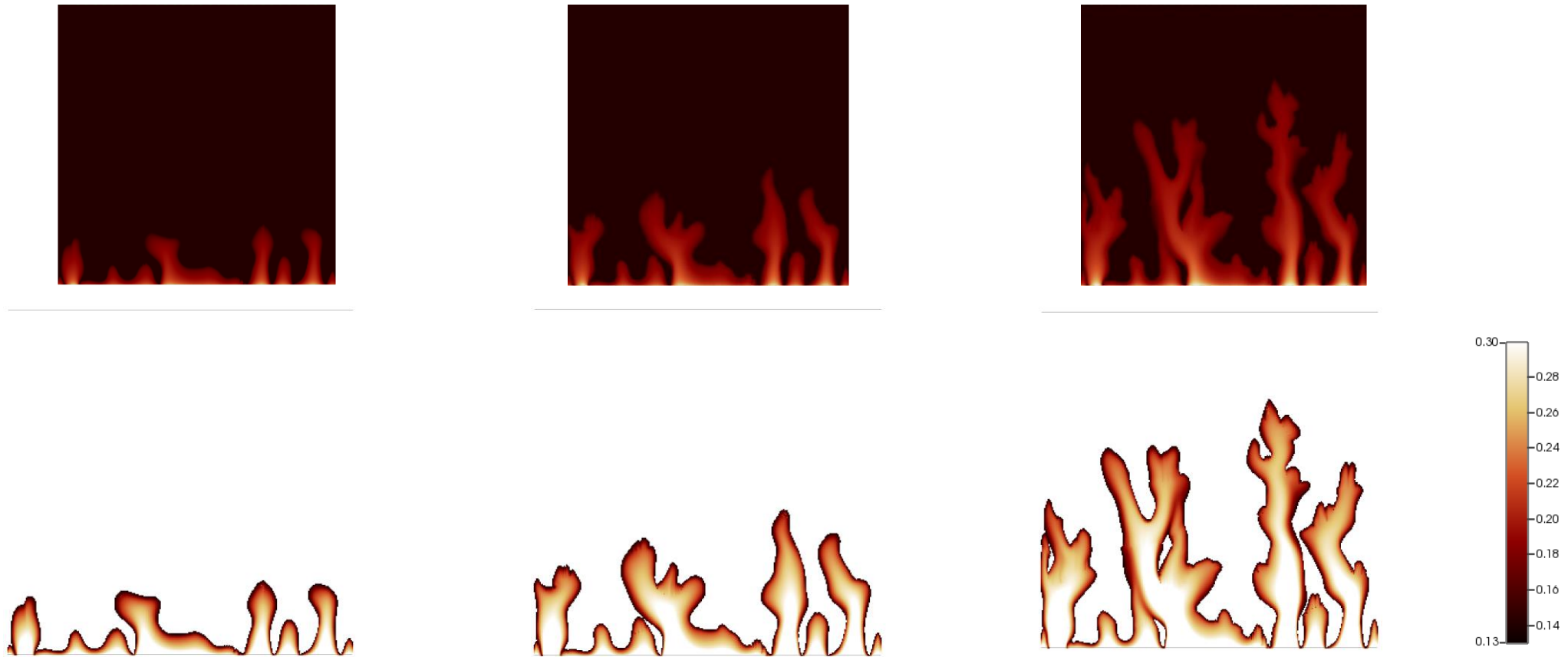
0.14 PV   0.53 PV   2.3 PV

Analysis of water saturation in water fingers

Average Saturation @ the front in the finger:
$S_w = 0.20$

Observations

Fractal type fingers is formed at early stage of the waterflood

Early breakthrough of water (0,04 PV) 2000:1

Fingers is broadened and the stronger fingers progress

Fingers collapse into channels at later stage

Direct Simulation of Viscous Fingering –Literature Examples
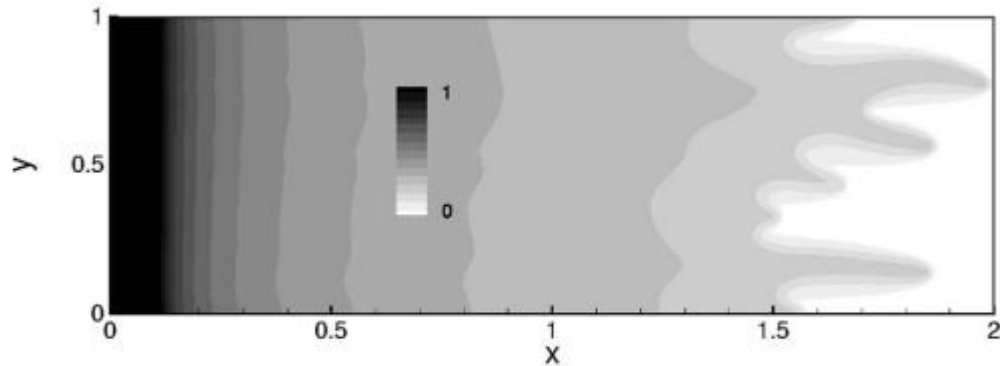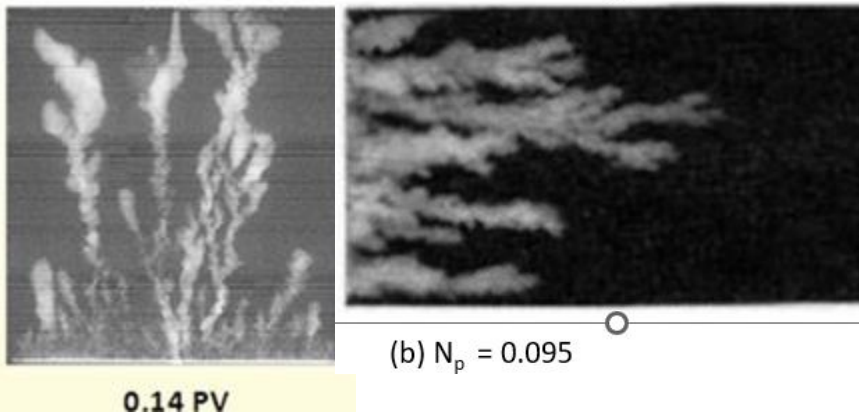
(Riaz & Tchelepi, 2006, Phys. Fluids)

FIG. 7. Full saturation profile in a fixed reference frame for $M=100$, Ca $=100$ and $A=2$ at $t=0.2$. Viscous fingers are localized around the front. The region behind the front does not experience instability. The growth rate of viscous fingers is small compared to the front speed.

NOTHING LIKE …

(b) $N_p = 0.095$

0.14 PV

Riaz & Tchelepi noted ..
"Although the … fingers obtained by our simulation are qualitatively similar to experimental observations,… *the amplitude of fingers is somewhat inconsistent with experimental results, where the length of viscous fingers is much larger.*"

"One possibility for this difference could be ..**the relative permeability (RP) and capillary functions** used in our analysis are different from the actual form of these functions in the experiments."

(Riaz & Tchelepi, 2006, TIPM)
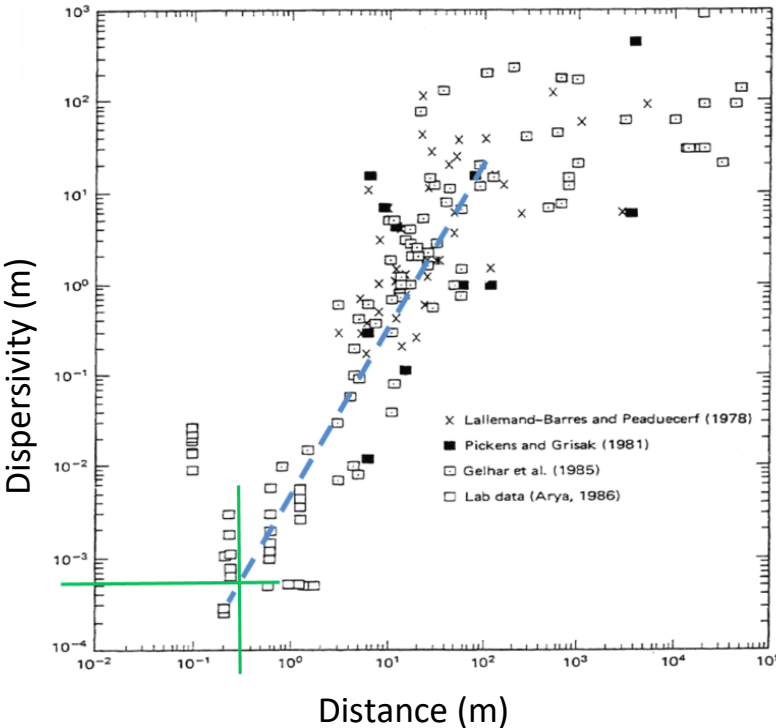Followed up above (broadly correct) conjecture and showed that RPs were definitely involved … but still did not obtain fully developed viscous fingers .

Reservoir engineering approach (4 Step model)

1. Grid size, Choose sufficiently fine spatial grid for numerical simulations

2. Random correlated permeability field

3. Chosen fractional flow function, $f_w^{*,}$, with a higher "shock front" saturation, S_{wf}^*, than found in conventional relative permeabilities.

4. Maximize the total mobility function, $\lambda_T = \lambda_O + \lambda_W$
The "correct" set of RPs which minimizes the pressure drop across the fingering system (least resistance)

Guidelines from dispersivity →
Low viscosity ratio - coarser grid
High viscosity ratio – finer grid

Example
Model Length: 0.3 m = 30 cm
Dispersity is estimated to: 0.05 cm
Cell length becomes: 2 x α_L=0.1 cm

Dispersivity (m) vs Distance (m)

X Lallemand–Barres and Peauducerf (1978)
■ Pickens and Grisak (1981)
☐ Gelhar et al. (1985)
☐ Lab data (Arya, 1986)

Model length	Approx. Grid size
meter	mm
100 m	dm
1000 m	m
10 km	10 m

Permeability Fields (Correlated Random Fields, CRF)
$(k_{lo} = 10\ mD,\quad k_{hi} = 1000\ mD)$ *Varying correlation length*

$\lambda_D = 1/10$ $\lambda_D = 1/30$ $\lambda_D = 1/100$

Permeability Fields (Correlated Random Fields, CRF)
$(k_{lo} = 10\ mD\ ,\quad k_{hi} = 1000\ mD)$

(a)

(b)
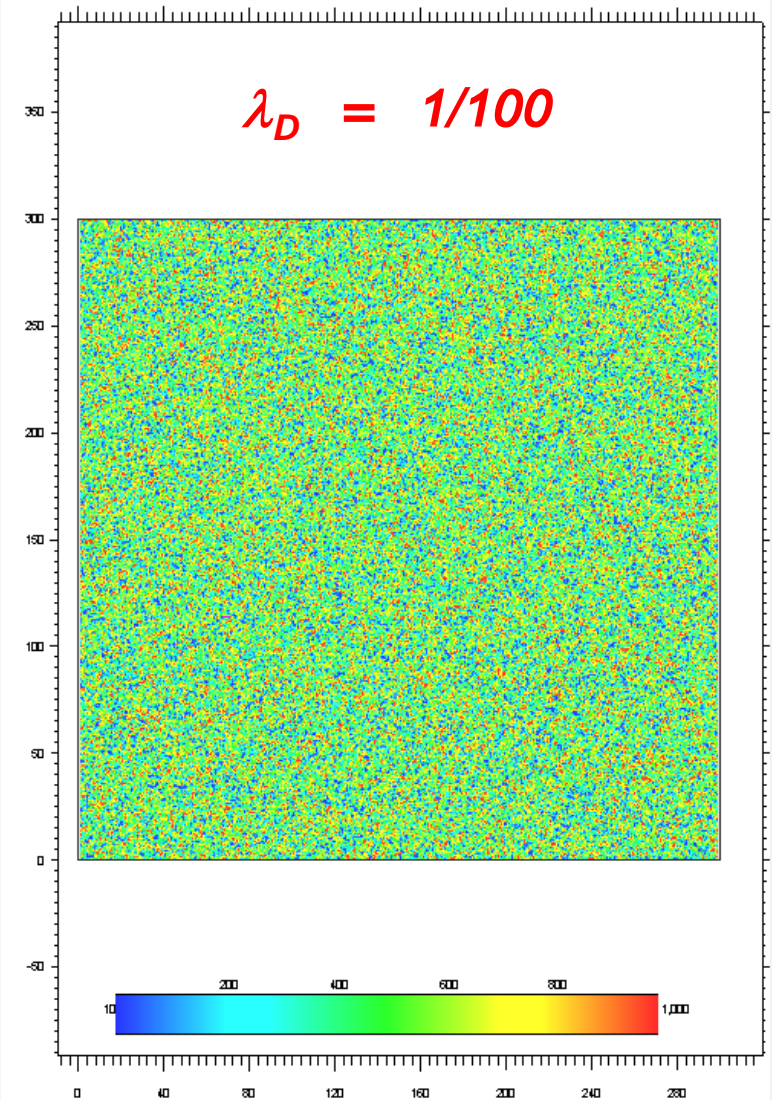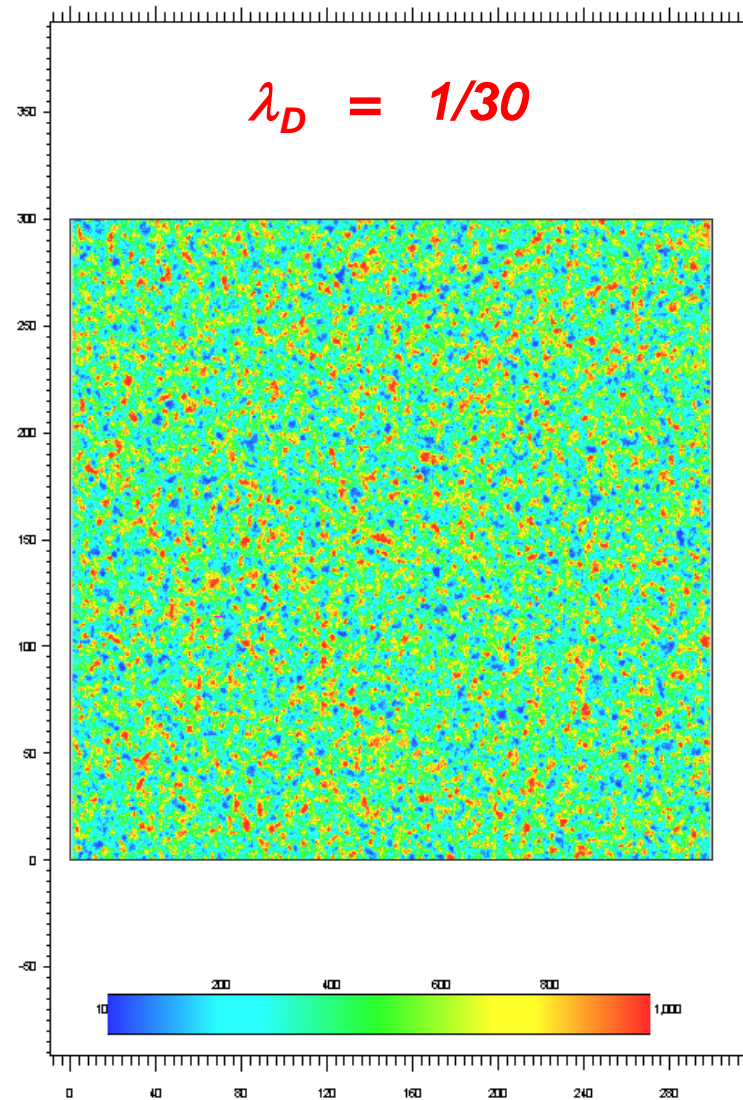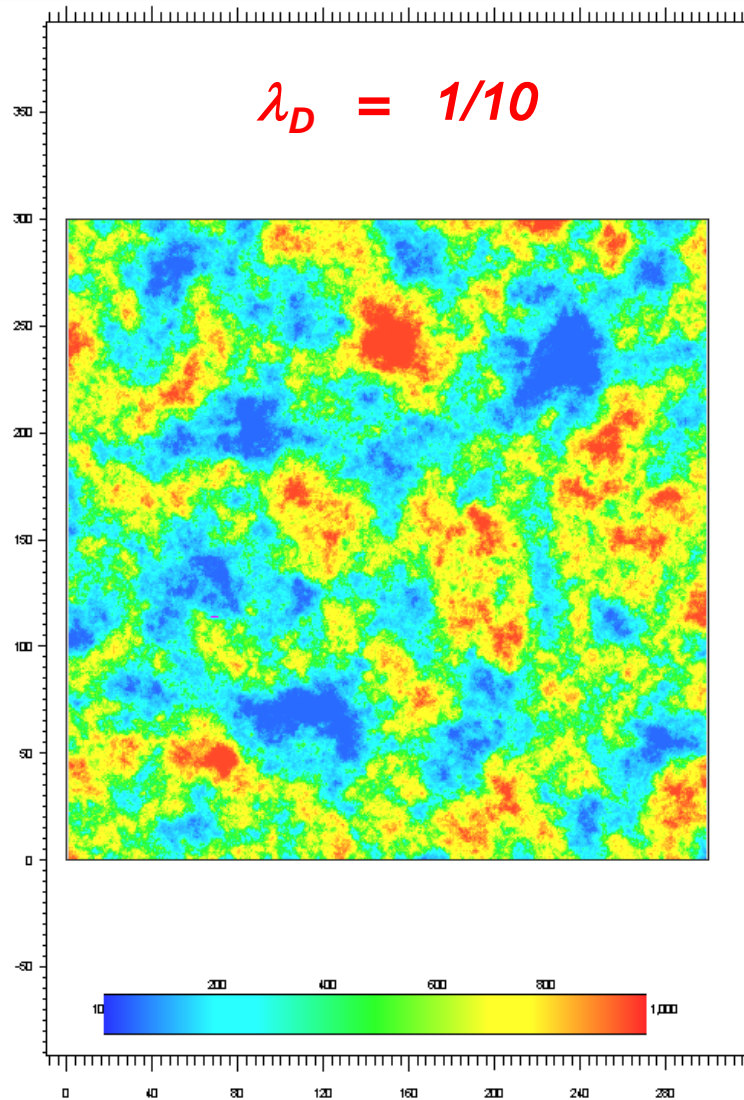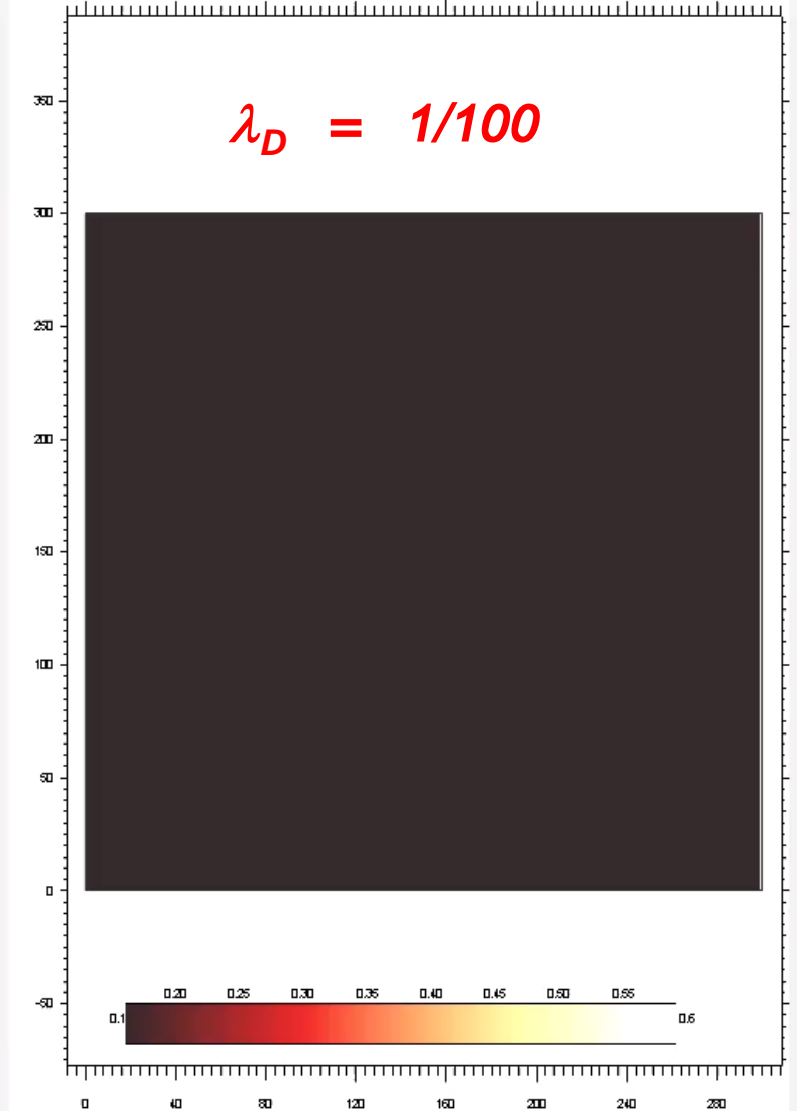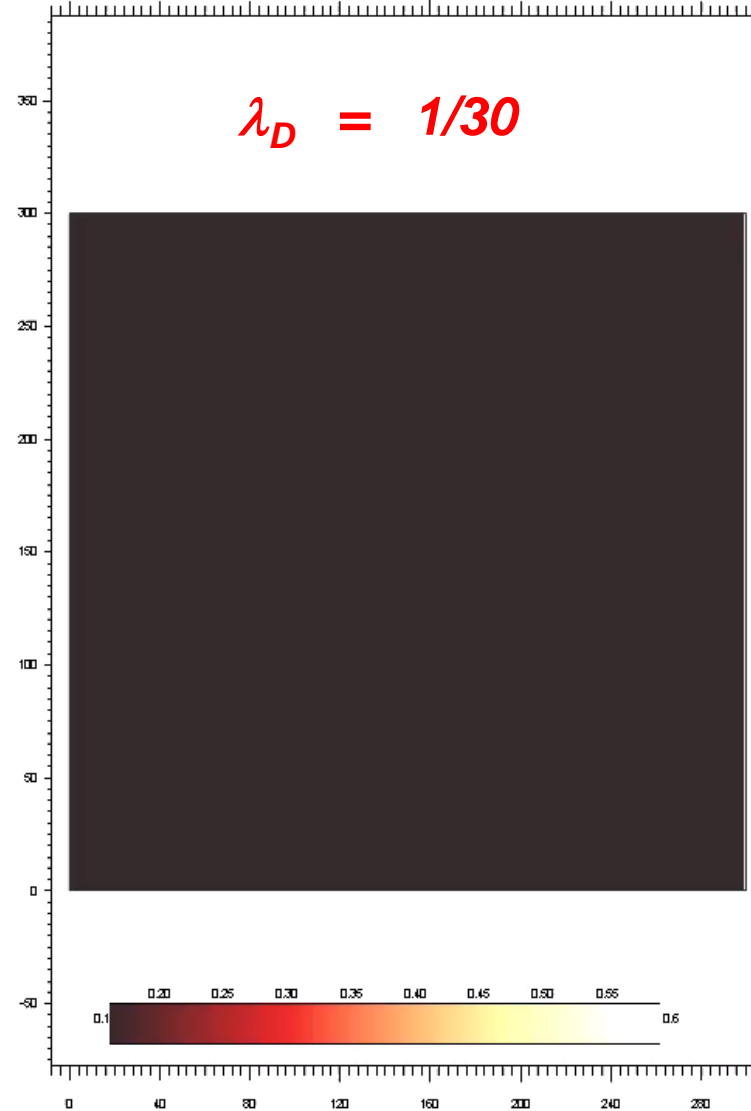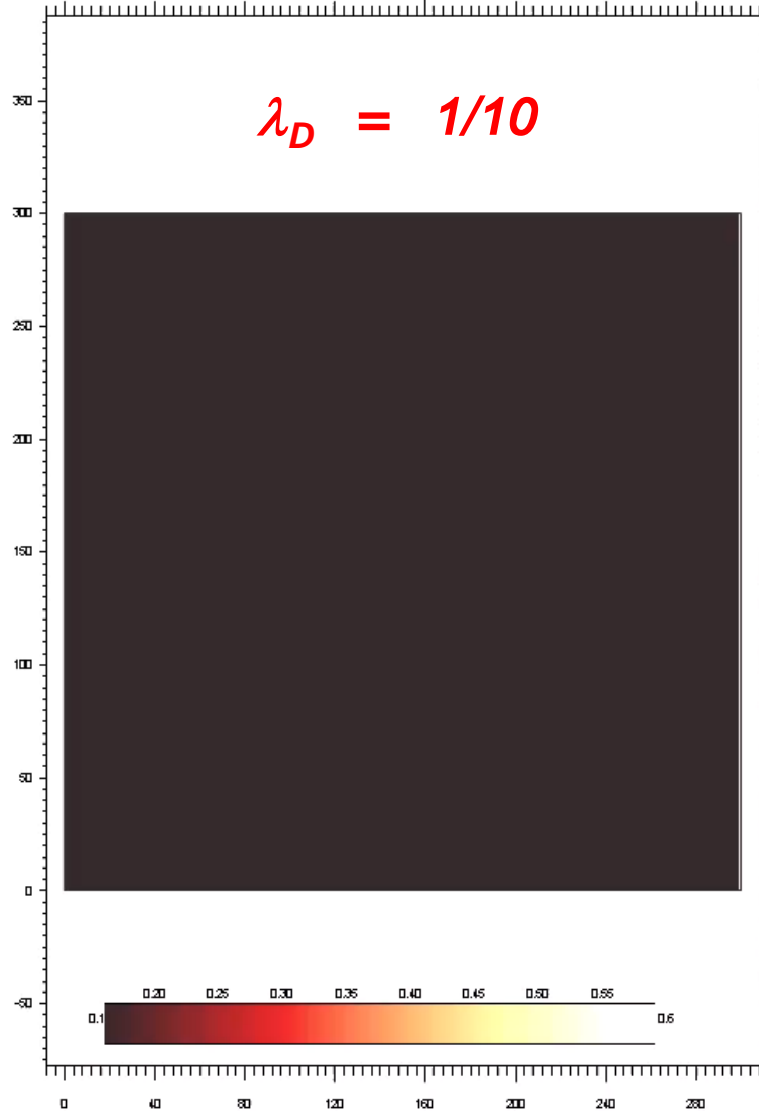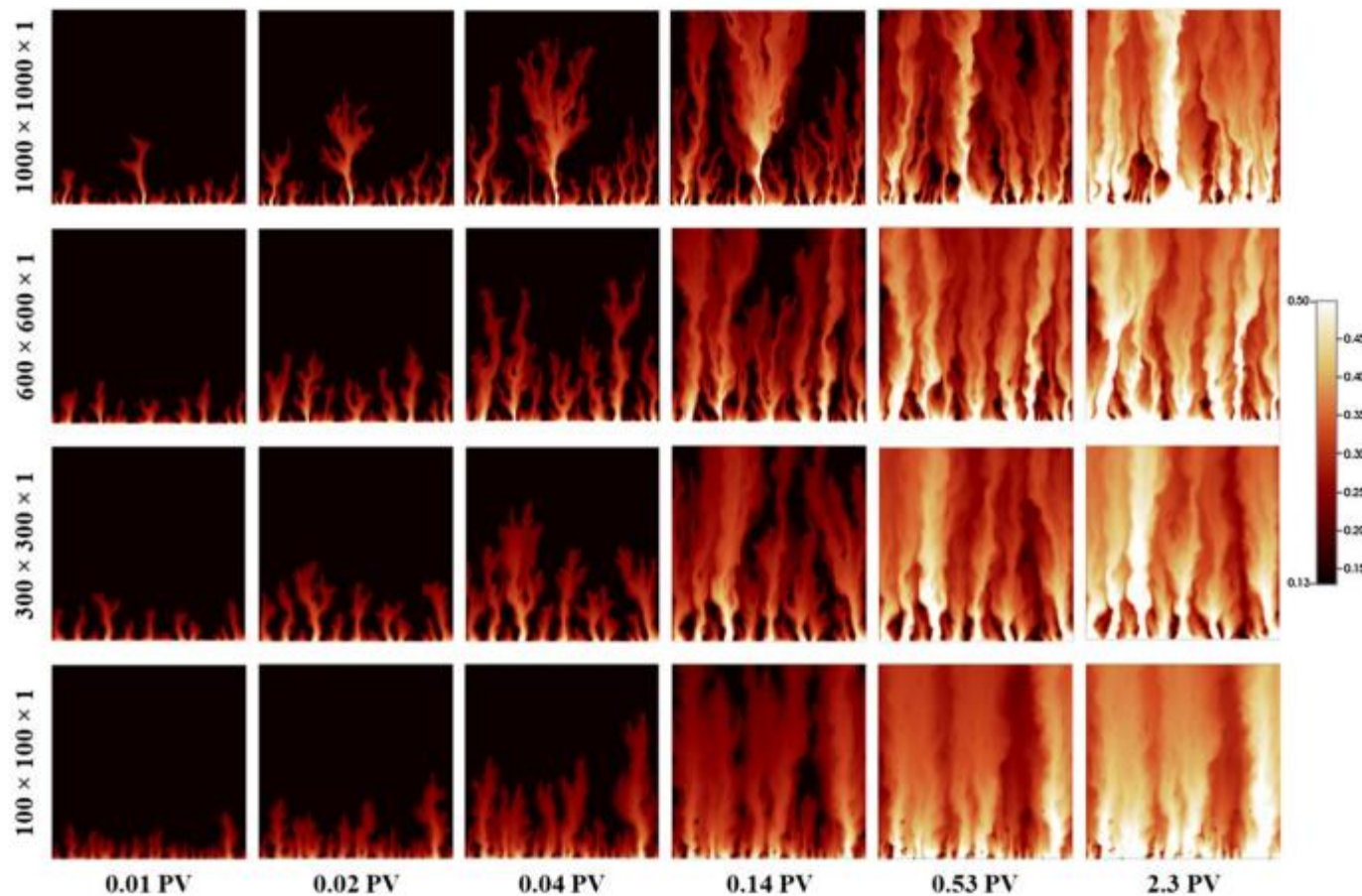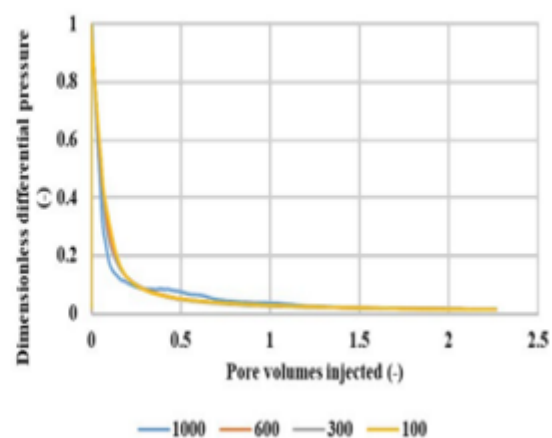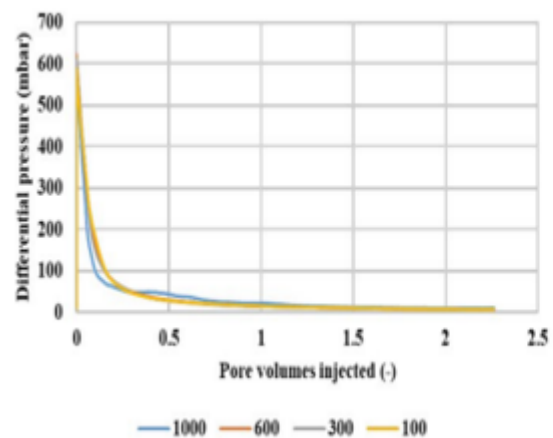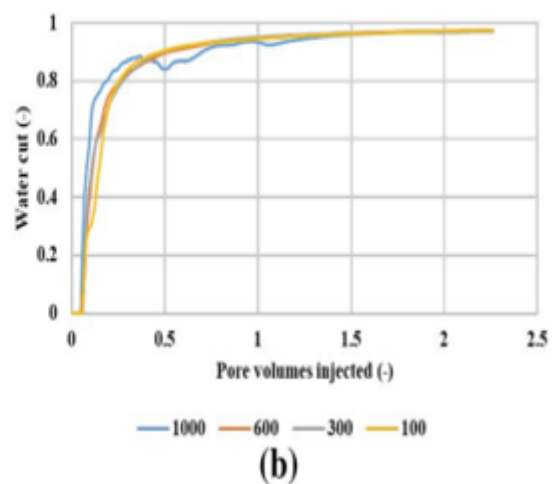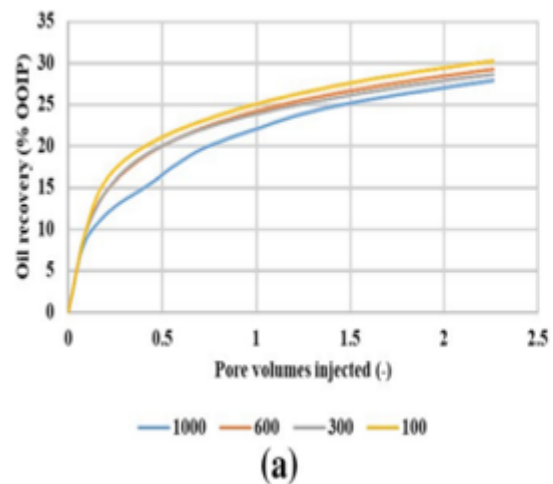
Thinner fingers with finer grid but,
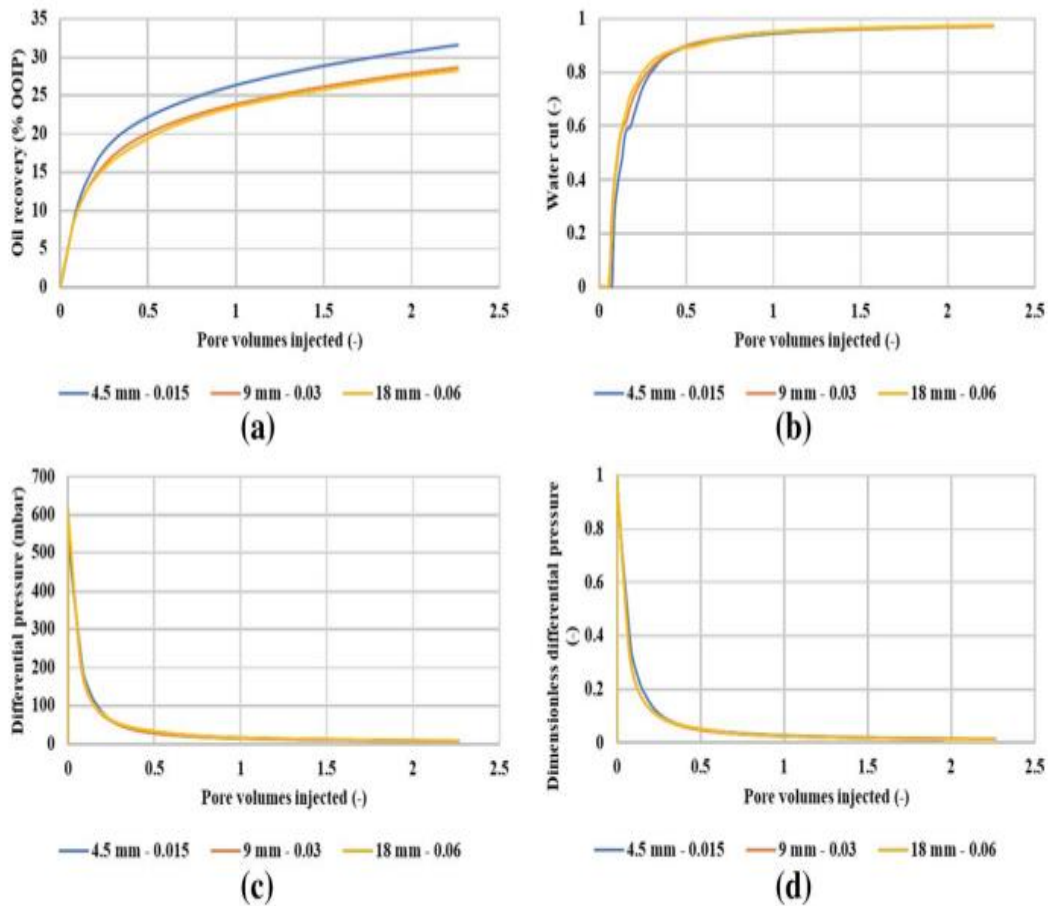More fingers grow to become large fingers in coarser grid giving a somewhat later water BT

Fig. 7 **a** Oil recovery, **b** water cut, **c** differential pressure and **d** dimensionless differential pressure for the three correlation length cases in the correlation length sensitivity study
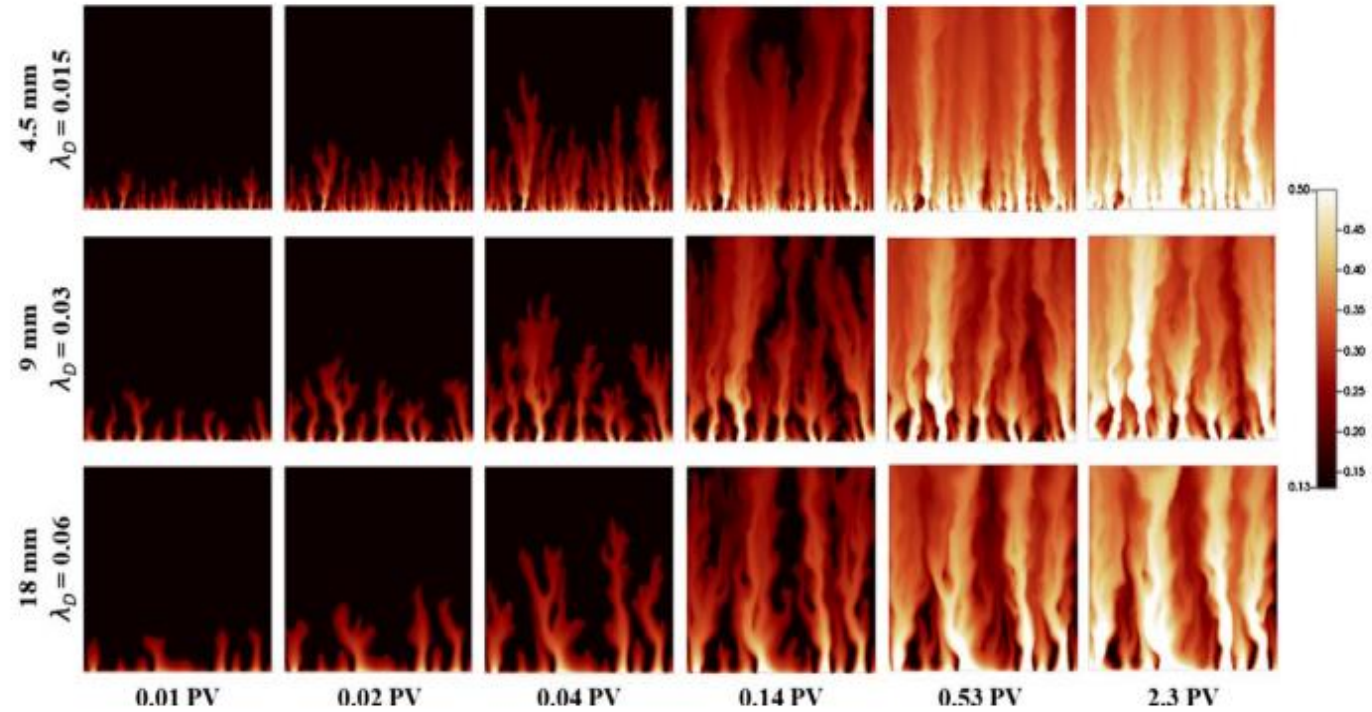

Fig. 8 Local water saturation development at different pore volumes injected for grid with size $300 \times 300 \times 1$ with random correlated permeability field with dimensionless correlation length of 0.015, 0.03 and 0.06

Guidelines: Dimensionless correlation length 0.03 – 0.06 seems ok, Actually $0.03 < \lambda_D < 0.1$ is ok in these cases

Step 3 and 4 Fractional flow and total mobility

The relation between relative permeability and fractional flow, fw*, at any given saturation (Sw) is given by

$$\left(\frac{k_{ro}^*}{k_{rw}^*}\right) = \left(\frac{\mu_o}{\mu_w}\right)\left(\frac{1}{f_w^*(S_w)} - 1\right)$$
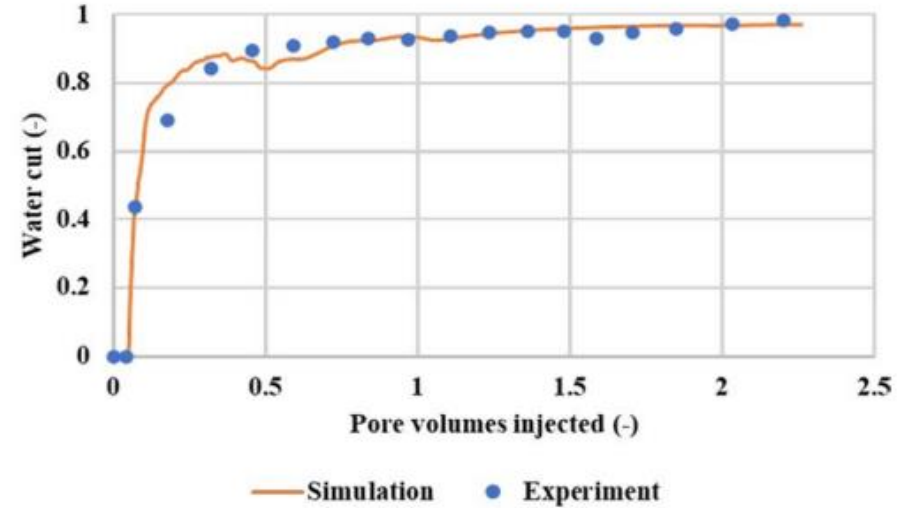
Once the fractional flow is chosen to honor the saturation in the fingers, the ratio of relative permeabilities is given but the individual curves are chosen such that the total mobility, is maximized.
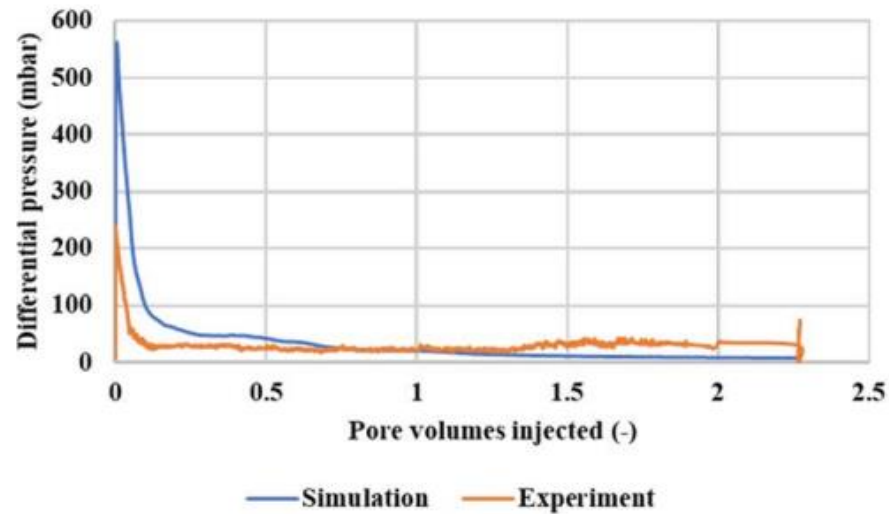
$$\lambda_T = \lambda_o + \lambda_w$$
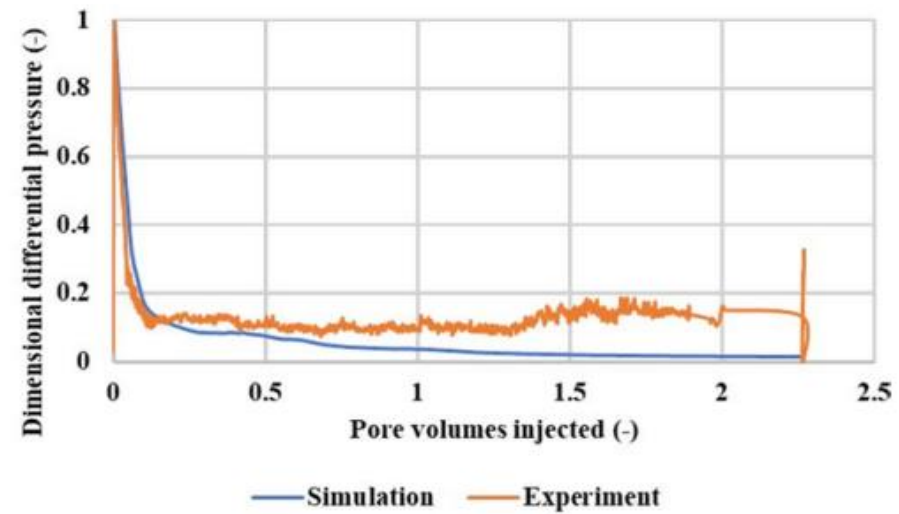
Example 2000 cP
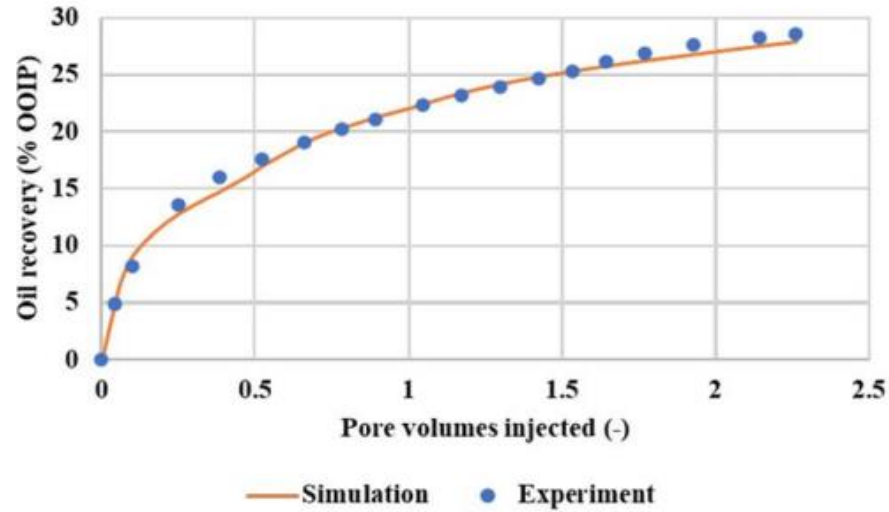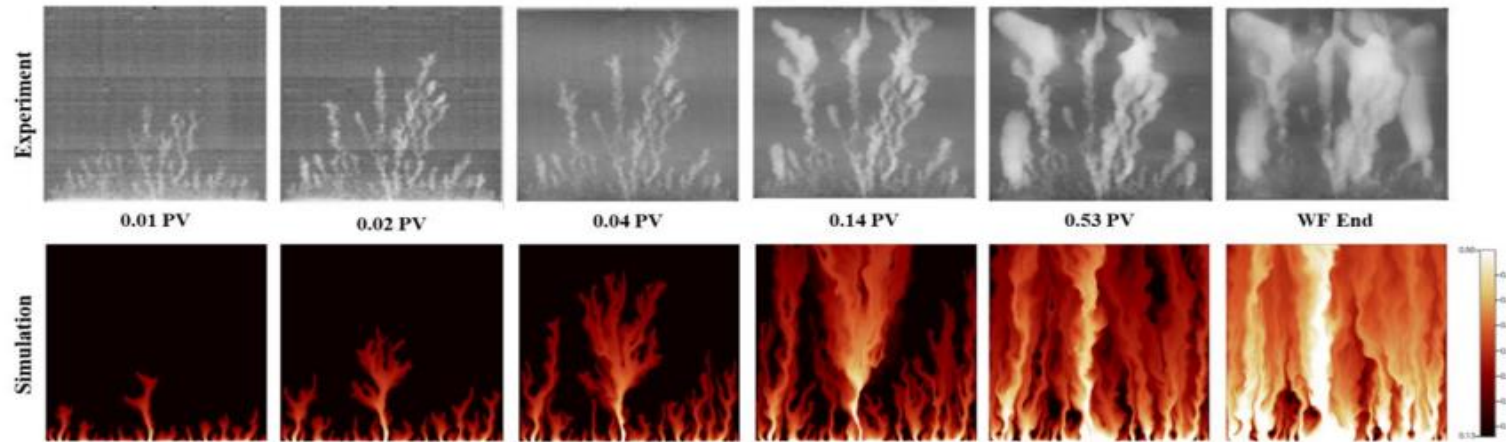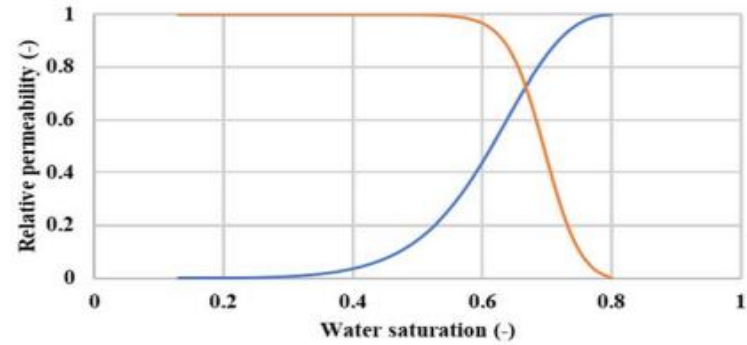

Experimental data and simulated **a** Oil recovery, **b** water cut, **c** differential pressure and **d** dimensionless differential pressure for the $\mu_o = 2000$ cP case
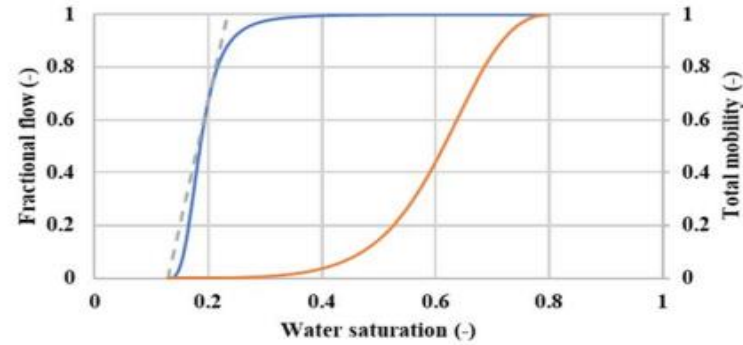
Viscous fingering estimates

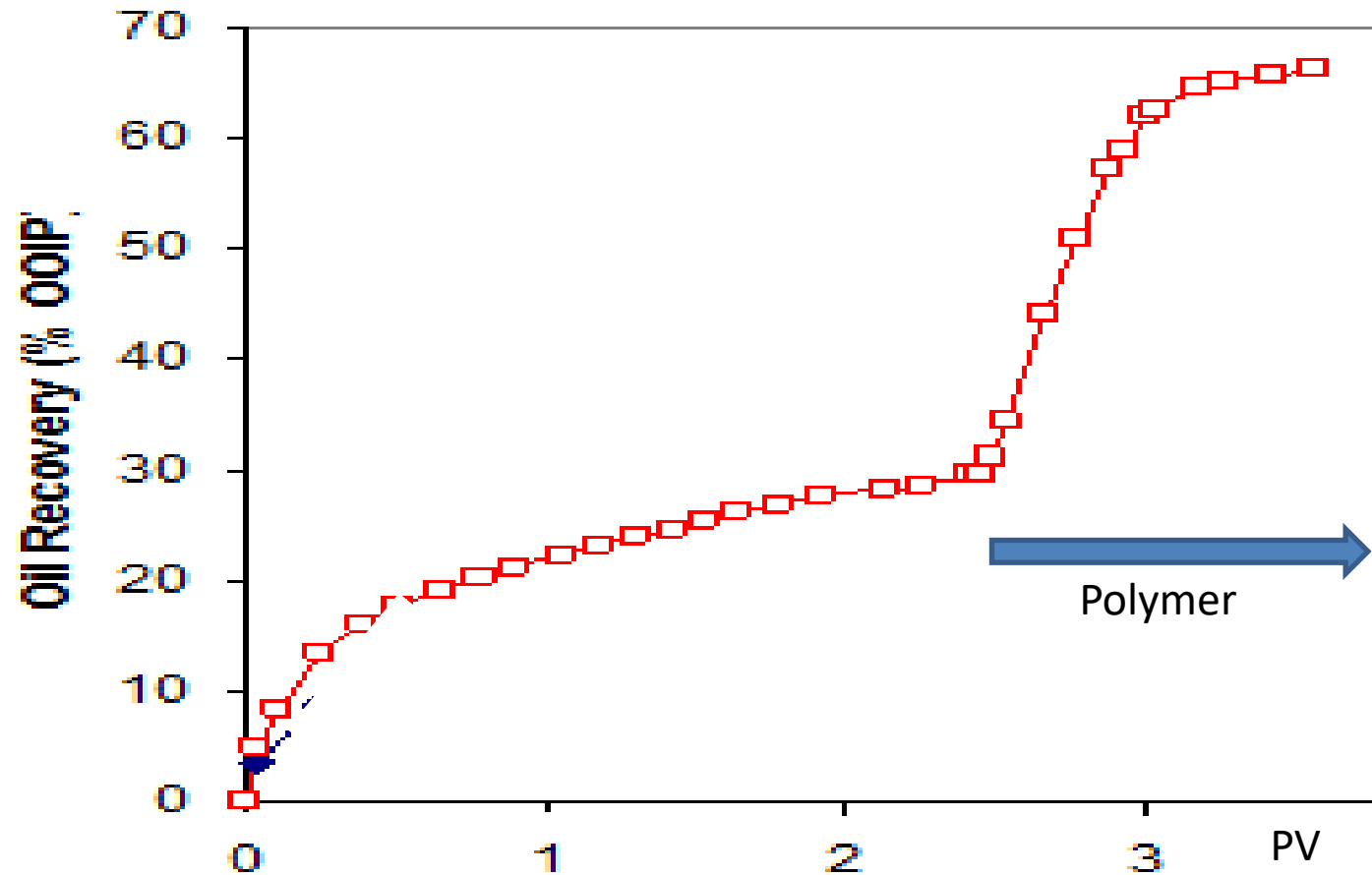Finger development during water injection for the $\mu_o = 2000$ cP experiment and the corresponding simulated match

The method gives Good match up to water breakthrough

a relative permeability curves and b fractional flow and total mobility for the simulated match of the $\mu_o = 2000$ cP experiment

Water- and polymer flood

Polymer both increase oil recovery and accelerate production

Oil mobilization during polymer flood
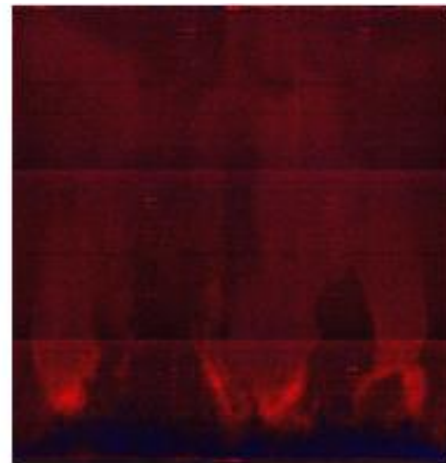
X-ray camera visualize change in oil and water saturation
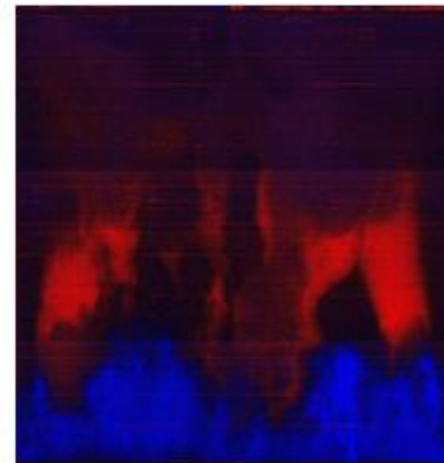
E2000   Change in saturations after end of waterflood
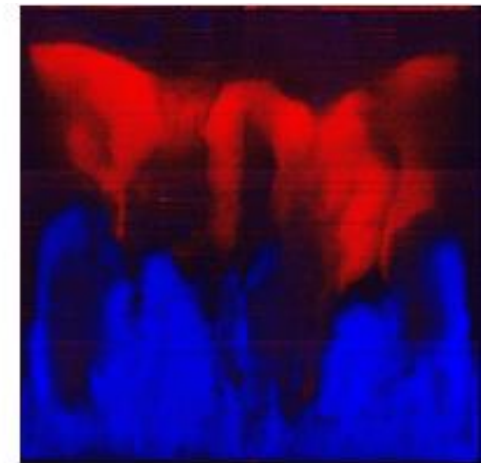
Ref. end of waterflood   0.02 PV   0.11 PV   0.25 PV

Red: increased oil saturation
Light blue: increased water saturation

Early oil mobilization through established water channels
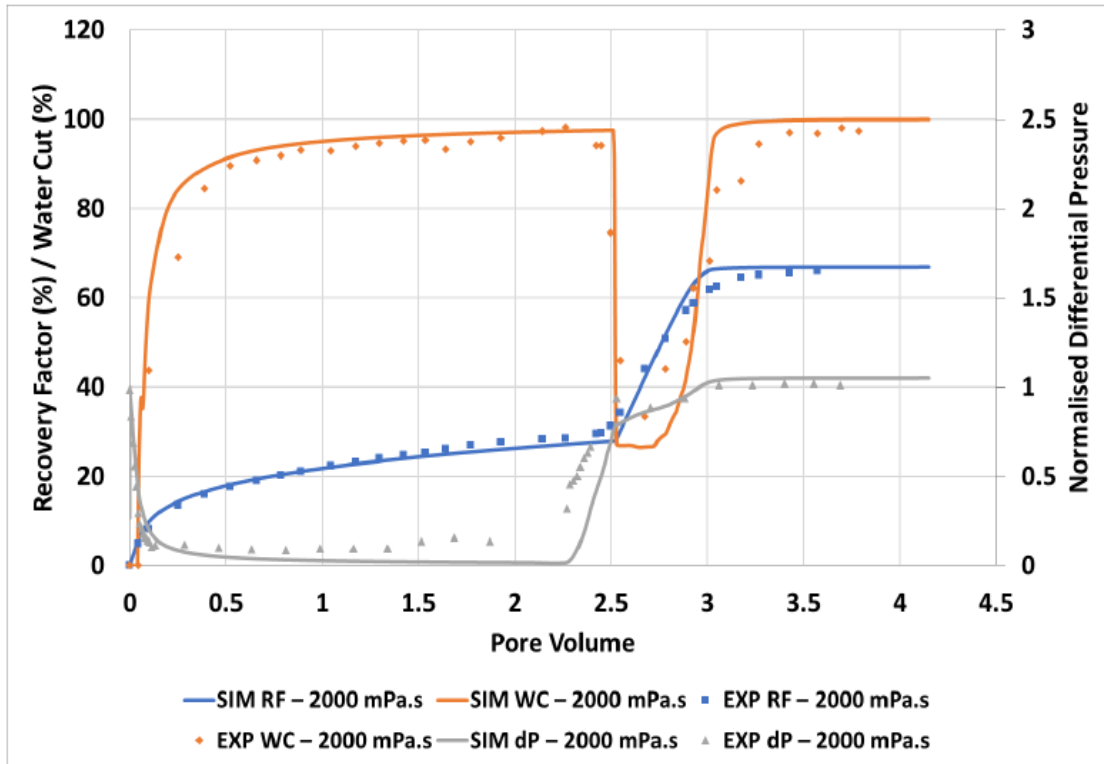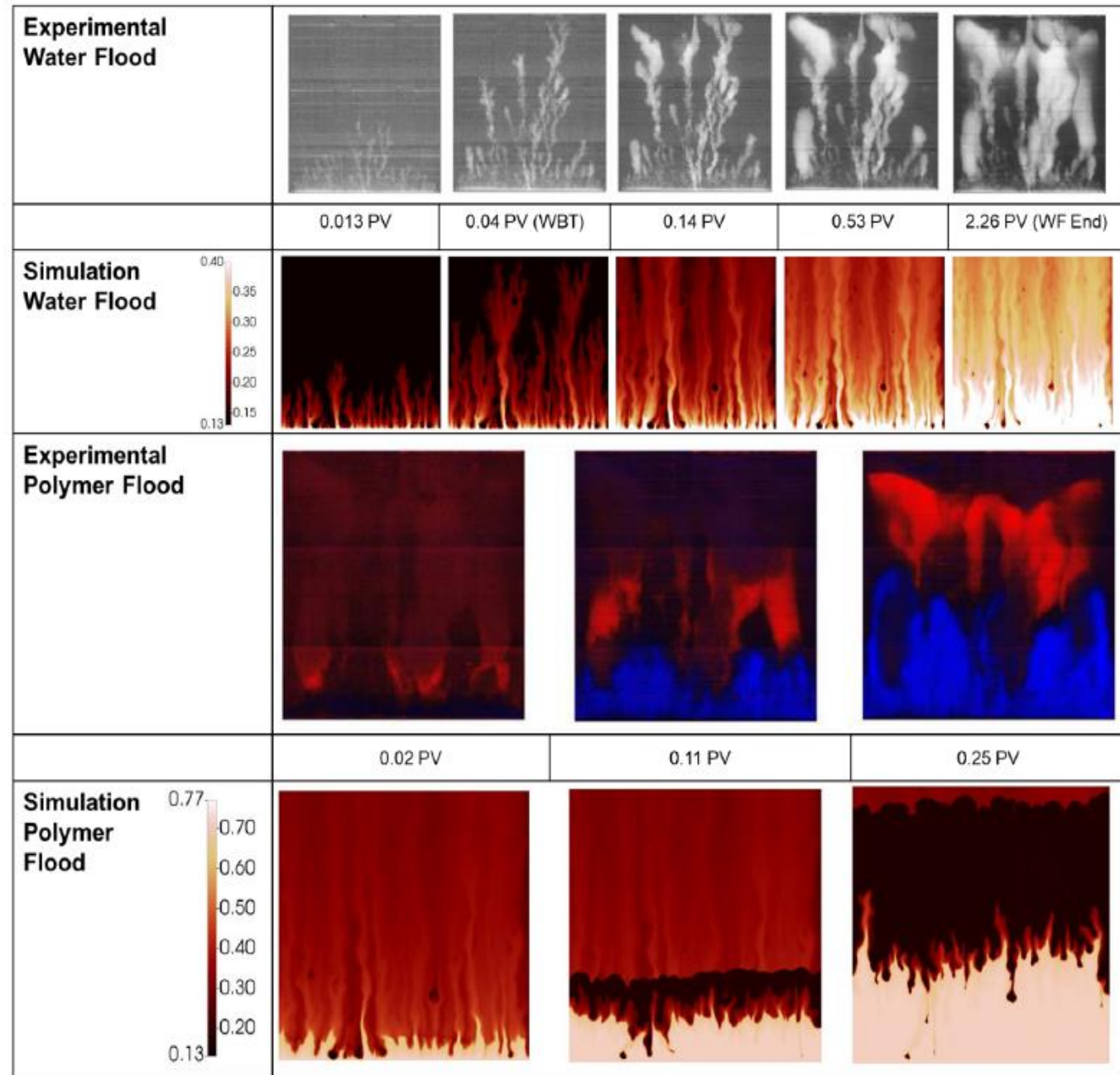
Polymer flood modelling

Figure 4. Simulation match of the unstable displacement of 2000 mPa.s oil.

CONCLUSIONS

Modeling immiscible viscous fingering anchored on experimental data on water displacing viscous oils.

In all experiments modelled, from very good to excellent agreement is found when comparing the direct numerical modelling and experimental results for all quantities measured, including the production and differential pressure profiles (vs. PV) as well as the specific characteristics of the finger patterns themselves.

Starting from the fractional flow, which gives the correct water saturations in the fingers, and then working back to the underlying relative permeabilities giving the maximum total mobility while still honoring the chosen fractional flow function.

Analysing tertiary polymer floods strongly support the view that the polymer works by 2 main mechanisms;

(a) enhanced viscous linear displacement (or extended Buckley-Leverett (BL) mechanism
(b) by an additional viscous crossflow (VX) mechanism

Acknowledgment to JIP sponsors:

Chair acknowledge cooperation with:

¡THANKS!

// STAVANGER 2022
ANNUAL EVENT

eor
Enhanced Oil Recovery

Technology
Collaboration
Programme
by iea